STAR Protocols

CellPress
OPEN ACCESS

Protocol

Using fluorescent indicators for *in vivo* quantification of spontaneous or evoked motor neuron presynaptic activity in transgenic zebrafish

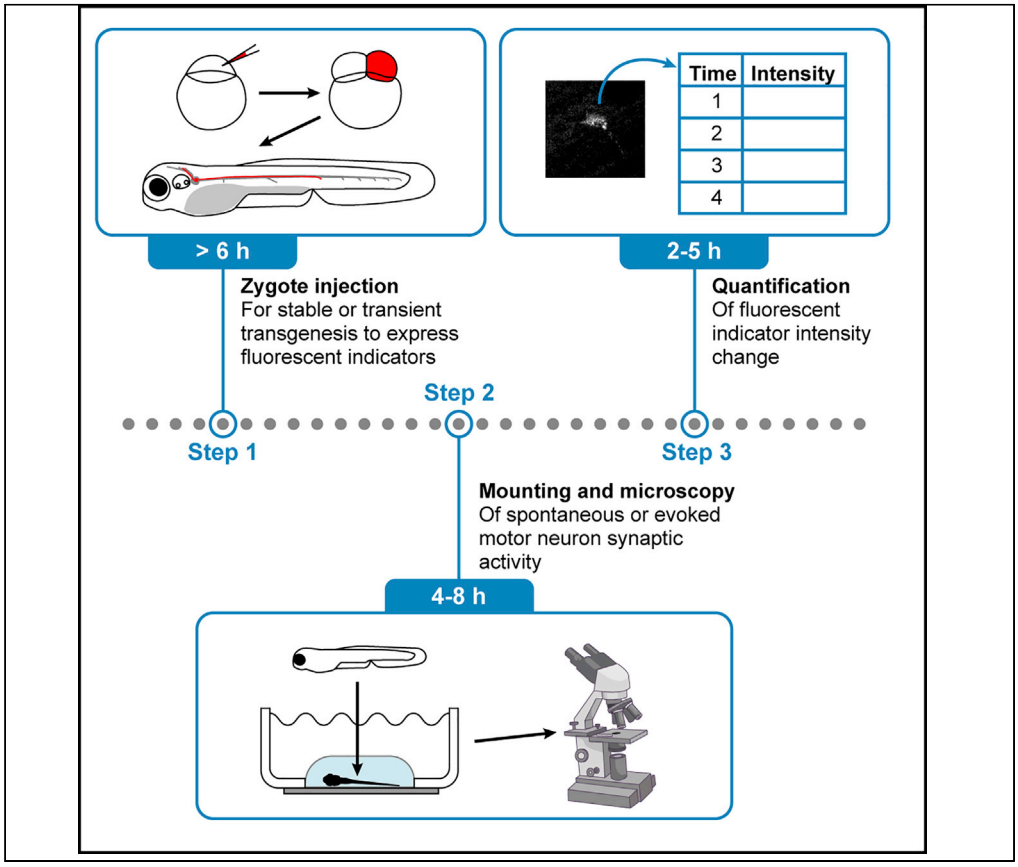

In this protocol, we describe steps that utilize the optical clarity of the zebrafish larvae and the stereotyped motor neuron axon structure in the trunk to measure spontaneous or evoked motor neuron axon activity. This activity is detected with transgenic fluorescent indicators introduced into the larvae by zygotic injection. Fluorescent indicator intensity changes in the small neuromuscular junctions are quantified to measure the presynaptic calcium activity and consequent synaptic vesicle release.

Publisher's note: Undertaking any experimental protocol requires adherence to local institutional guidelines for laboratory safety and ethics.

Hiu-tung Candy Wong, Catherine M. Drerup

hcwong3@wisc.edu (H.-t.C.W.)
drerup@wisc.edu (C.M.D.)

Highlights

Zebrafish zygote injection to express fluorescent indicators in the motor neuron

Imaging of motor neuron presynapse for synaptic vesicle release or calcium influx

Image acquisition during spontaneous and evoked motor neuron synaptic activity

Quantification of indicator fluorescence intensity in spontaneous or evoked activity

Wong & Drerup, STAR Protocols 3, 101766 December 16, 2022
https://doi.org/10.1016/j.xpro.2022.101766

STAR Protocols

CellPress
OPEN ACCESS

Protocol

Using fluorescent indicators for *in vivo* quantification of spontaneous or evoked motor neuron presynaptic activity in transgenic zebrafish

Hiu-tung Candy Wong[1,2,*] and Catherine M. Drerup[1,3,*]

[1]Department of Integrative Biology, University of Wisconsin-Madison, Madison, WI 53706, USA

[2]Technical contact

[3]Lead contact

*Correspondence: hcwong3@wisc.edu (H.-t.C.W.), drerup@wisc.edu (C.M.D.)
https://doi.org/10.1016/j.xpro.2022.101766

SUMMARY

In this protocol, we describe steps that utilize the optical clarity of the zebrafish larvae and the stereotyped motor neuron axon structure in the trunk to measure spontaneous or evoked motor neuron axon activity. This activity is detected with transgenic fluorescent indicators introduced into the larvae by zygotic injection. Fluorescent indicator intensity changes in the small neuromuscular junctions are quantified to measure the presynaptic calcium activity and consequent synaptic vesicle release.

For complete details on the use and execution of this protocol, please refer to Mandal et al. (2020).

BEFORE YOU BEGIN

Zebrafish larval skeletal motor neurons

At 4 days post-fertilization (dpf), the zebrafish can already swim, escape from a variety of stimuli, and engage in visually guided predation (Budick and O'Malley, 2000). The zebrafish spinal motor neurons are an important component of the neural circuitry. They receive input from reticulospinal neurons such as Mauthner cells and interneurons to control these swimming and startle behaviors (Bernhardt et al., 1990; Hale et al., 2001; Jontes et al., 2000). The larval zebrafish spinal motor neurons can be separated into two morphological classes—primary and secondary, which begin development at around 1 dpf (Bernhardt et al., 1990; Eisen et al., 1986; Myers et al., 1986). Importantly for our methods, primary motor neurons have larger axons and are therefore easier to visualize than axons of secondary motor neurons (Bello-Rojas et al., 2019; Menelaou and McLean, 2012; Myers et al., 1986). The morphology of motor neurons can be correlated to functional differences—larger motor neurons tend to innervate larger and more muscle fibers and together deliver strong but transient forces (Fetcho, 1992; Heckman and Enoka, 2012). In contrast, a subset of motor neurons that deliver weaker but sustained forces are inhibited during these strong movements such as in fictive swimming (Kishore et al., 2014; Menelaou and McLean, 2012).

Primary motor neurons can be further classified as Middle primary (MiP), Rostral primary (RoP), and Caudal primary (CaP), which differ mainly by the stereotyped peripheral arbor innervating distinct muscular targets (Bello-Rojas et al., 2019; Bernhardt et al., 1990; Eisen et al., 1986; Myers et al., 1986). We selectively image CaP motor neuron axons in this protocol due to their superficial location and easily recognized peripheral arbor: unlike the RoP and MiP, the axon of the CaP extends ventrally, in the space between the notochord and the medial surface of the muscles, past the horizontal myoseptum, to the ventral edge of the musculature, then turns dorsally and laterally to project over the lateral surface of the muscle (Figures 1A and 1B).

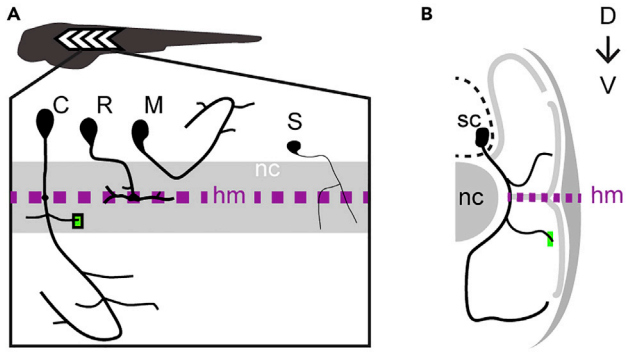

Figure 1. Anatomy of zebrafish larval motor neurons

(A) Schematic of the trunk in the sagittal plane showing the position of the notochord (nc), horizontal myoseptum (hm, purple dotted line). Primary motor neurons CaP (C), RoP (R), MiP (M) axons, and secondary motor neuron (S) axon show distinct arborization and axon width. Green rectangle shows an example segment of CaP axon from which synaptic activity may be quantified.

(B) Transverse plane showing primary motor neuron extending from the spinal cord (sc). CaP axon (black solid line) is differentiated from RoP and MiP axons (gray solid line) by its extension past the hm, to the ventral edge of the musculature. Superficial branches of the CaP axon near the hm are recommended for imaging using this protocol. Green rectangle shows the lateral view of the example CaP axon segment of interest.

Anesthetizing zebrafish larvae for live imaging

For live imaging, zebrafish larvae must be immobilized. The typical method for anesthetizing zebrafish is through bath application of tricaine (also known as MS-222 or MESAB). This allows efficient immobilization of larvae and is used for positioning larvae in agarose during mounting. However, tricaine should be removed prior to imaging because its function as a sodium channel blocker will alter the membrane electrical property of the neurons in the sensorimotor circuit. Larvae recover from tricaine exposure swiftly and typically regain motility within 1 min after wash-out. For this reason, the larva is immobilized by low-melt agarose alone or with the paralytic α-bungarotoxin during imaging in this protocol. α-bungarotoxin blocks the nicotinic acetylcholine receptor (nAChR) which is required in the muscle post-synapse to trigger contraction but has no effect on the pre-synapse (Berg et al., 1972; Chang and Lee, 1963; Lee et al., 1967; Miledi and Potter, 1971). Therefore, α-bungarotoxin can inhibit larval movement without blocking motor neuron function.

Stable and transient transgenesis

Stable transgenesis to create zebrafish strains with cell-type specific expression of fluorescent reporters is an important technique for zebrafish research. A stable transgenic zebrafish line is created through the insertion of exogenous DNA into the genome and subsequent germline transmission of the transgene. Insertion of transgenic DNA into the genome can be achieved with available molecular tools such as the Tol2 transposable element used in the Tol2kit, followed by identification and propagation of offspring resulting from edited gametes (Kwan et al., 2007). Because the copy number and location of the transgene within the genome are consistent, a stable transgenic line shows predictable expression levels between siblings and generations, discounting epigenetic modification. Stable transgenesis is useful for experiments where uniform expression of the transgene within the targeted cell types is desired (Mandal et al., 2020; Zhao et al., 2011). In this protocol, the calcium indicator G-GECO is expressed in a stable transgenic line (*Tg(5kbneurod:G-GECO)*^{n119}; (Mandal et al., 2018)).

Conversely, transient transgenesis allows the expression of fluorescent reporters under cell-type specific promotors in a single generation and does not require stable insertion of the transgene into the genome. Transient transgenesis is achieved by introducing transgenes into zebrafish zygotes through the microinjection of plasmid DNA. Because exogenous DNA is mosaically inherited during cell division, there is a stochastic expression of the transgene in injected embryos. Transient

transgenesis is useful for many experiments when sparse expression is desired or for efficiency as making a stable line requires several months. Experiments involving quantitative comparisons of fluorescence intensity using transient transgenesis must be carefully controlled because the transgene copy number is not identical between cells within the same animal or between animals, unlike stable transgenics. To compare fluorescence intensity changes, it is ideal to normalize signal intensity to an internal control. In this protocol, fluorescent intensity comparison of pHluorin fused to synaptophysin (SypHy), a pH-sensitive indicator of synaptic vesicle release, is feasible because of the ratiometric expression of cytoplasmic mRFP through a P2A cleavable peptide (Campbell et al., 2002; Kim et al., 2011). The inclusion of a 2A peptide sequence causes a co-translational, autoproteolytic cleavage to yield SypHy and mRFP (Liu et al., 2017; Ryan and Drew, 1994). While SypHy fluorescence is dependent on rate of exocytosis, mRFP fluorescence intensity can be correlated to its expression level. Therefore, mRFP can be used as a normalizing factor for SypHy expression levels in the same cell. This ratiometric analysis of SypHy signal accounts for the variable transgene expression between cells and animals. In this protocol, the mnx1 promoter is included in the 5′ region of the transgene to drive neuron-specific SypHy expression. However, UAS:SypHy may instead be injected into zygotes with the appropriate tissue specific stable transgenic Gal4 expression (Almeida et al., 2021).

Plasmid generation

Plasmids for stable and transient transgenesis were generated using Gateway technology (Kwan et al., 2007). For analyses of motor neuron synaptic vesicle release, we generated a plasmid to express an exocytosis indicator protein SypHy, in motor neurons under the *mnx1* promotor (Flanagan-Steet et al., 2005; Miesenböck et al., 1998; Palaisa and Granato, 2007; Sankaranarayanan et al., 2000; Seredick et al., 2012). This plasmid contained a P2A cleavable peptide linking SypHy to mRFP (monomeric red fluorescent protein; *mnx1:SypHy-p2a-mRFP*). For analyses of calcium influx indicative of synaptic activity, we utilized G-GECO in a stable transgenic line (Zhao et al., 2011). Expression in this line is driven by a 5 kilobase (kb) portion of the *neurod* promotor which expresses in all neurons during and immediately after differentiation (*Tg(5kbneurod:G-GECO)*^{n119}). Due to the inherent variability of calcium imaging, it is recommended that this analysis is performed in a stable line.

Imaging system requirements

As technology advances, a growing number of microscopes and accessories are available for functional imaging of motor neurons. Here, important imaging system parameters are highlighted.

For imaging evoked motor neuron activity with the use of fluid jet stimulation, an upright rather than an inverted microscope and a dipping lens objective are strongly recommended. This allows easy access for fluid jet stimulation of the larva, which is submerged in embryo media. In contrast, the use of a coverslip is recommended for imaging spontaneous motor neuron activity, which may be performed on either an upright or inverted microscope. As no direct manipulation of the larvae is required, imaging through a coverslip is preferred as it allows for the use of an objective with a higher numerical aperture (NA) to achieve greater resolution.

The spatial and temporal resolution of the acquired time series images is an important consideration for imaging motor neuron synaptic activity. Primary motor neuron axons in zebrafish are approximately 2 μm in width (Myers et al., 1986). A 40–63× objective with an NA of 1.0–1.4 and a working distance of ~0.2 mm is likely suitable. The theoretical limit of resolving power in this setup ranges between 210–270 nm, which is sufficient to visualize the motor neuron axon and some subcellular features. For high-speed imaging, such as that described in the protocol for imaging evoked motor neuron activity, an electron multiplying charge-coupled device (EMCCD) or complementary metal-oxide semiconductor (CMOS) camera is generally used. For that, the pixel size of the detector should be considered. Generally, a microscope setup that can acquire images at 10 pixels per μm will be able to represent the width of the motor neuron axon with 20 pixels. For camera-based microscopes

such as the swept-field confocal, this would require a camera with a 6 μm pixel size (2 μm axon width × 60× magnification / 6 μm = 20 pixels). Pixel resolution is an especially important consideration for camera-based microscopes because spatial binning during imaging is likely required to adequately detect the emitted light. Spatial binning will reduce the number of pixels by half or a quarter (10 and 5 pixels, with the example above) that represent the width of the axon.

With regard to temporal resolution, the sections of this protocol which describes the imaging and analysis of spontaneous activity imposes fewer requirements than that of evoked activity. In this protocol, the rate of spontaneous motor neuron synaptic activity is assessed by measuring the sum of transient increases in fluorescent intensity in an area over time, which can be achieved by imaging for a longer time (minutes). For imaging evoked motor neuron synaptic activity, the exposure time range should adequately describe the rise time, and decay of the reporter fluorescent intensity back to baseline and depends on the rate of change of the fluorescence intensity. An adequate temporal resolution is helpful in informing the underlying reported synapse function and is important for distinguishing a genuine signal from the signal produced by technical artifacts such as movement. Motor neuron calcium flux was assessed using the calcium indicator G-GECO, which has a dissociation constant (K_d) of ~750 nM (Zhao et al., 2011). The duration of calcium signal is increased as K_d decreases. Generally, the decay signal depends on indicator kinetics, as well as the neuromuscular junction calcium clearance and buffering mechanisms. For this protocol, we recommend an exposure time of 100 ms or shorter to detect evoked synaptic response.

Institutional permissions

All work in this protocol was approved by the University of Wisconsin-Madison Animal Care and Use Committee. Readers will need to acquire permissions from the relevant institutions.

Prepare plasmid for zygotic microinjection

Timing: 3 days

Note: Maintain transgenic expression constructs by transforming circular DNA plasmids with antibiotic resistance into *E. coli* which is kept in glycerol stocks at −80°C for long term storage. We use the Tol2Kit to rapidly make expression construct plasmids (Kwan et al., 2007). Transient transgenesis is performed via microinjection of plasmid DNA only without the addition of Tol2 transposase mRNA used for generating stable lines.

1. Streak the −80°C glycerol stock on agar plates containing 100 μg/mL ampicillin. Incubate the plates at 37°C for 14–16 h.

   Note: Do not thaw the glycerol stock and immediately return the stock to −80°C after streaking.

2. Pick 2–4 colonies each into 3 mL of LB medium containing 100 μg/mL ampicillin and incubate at 37°C for 14–16 h in 220 rpm shaking.
3. Perform plasmids minipreps using the QIAprep Spin Miniprep kit following manufacturer's instructions with the following modifications: perform the optional PB buffer wash and elute in 30 μL deoxyribonuclease and ribonuclease-free water.
4. Check the plasmid sequence by digesting 2 μL of plasmid with the appropriate restriction enzyme (e.g., AlwNI for *mnx1:SypHy-p2a-mRFP* plasmid) and confirming that the digested fragments are the expected sizes using agarose gel electrophoresis. The appropriate restriction enzyme is dependent on the sequence of the expression plasmid, and the resolution of the method used to visualize the digested DNA fragments (e.g., with agarose gel electrophoresis, consider the percentage of agarose and the composition of the gel).

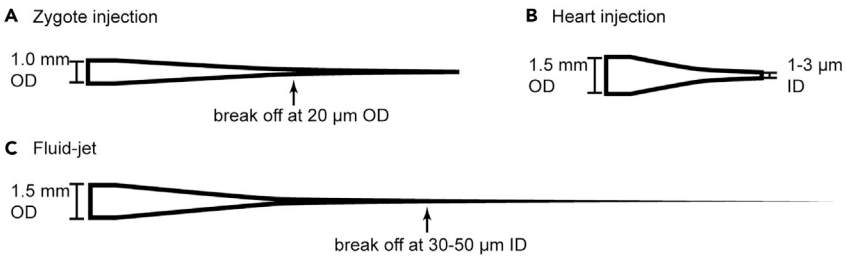

Figure 2. Glass capillaries are pulled into tapered needles for larval preparation and stimulation

(A–C) Unlike the zygote injection needle (A) and fluid-jet needle (C), which requires the tip to be broken off before use, the opening of the heart injection needle (B) is created while the capillary is pulled. Zygote injection needle opening size is estimated with a stage micrometer while heart injection and fluid-jet needles opening inner diameter are measured under a microscope. OD: outer diameter; ID: inner diameter.

5. Check the plasmid concentration with a spectrophotometer. The 260/280 nm absorbance ratio from 1.8 to 1.9 represent acceptably pure DNA plasmid sample. Plasmid concentration >150 ng/µL is preferred.

Pause point: Store the plasmid at −20°C indefinitely. Check the plasmid concentration and 260/280 ratio prior to use.

Prepare needles for injection and embryo manipulators

Timing: 1 h

6. Zygote injection needle: (Figure 2A) Prepare embryo injection needles by pulling a glass capillary with a filament (4 in length, 1.0 mm outer diameter) to create a tapered tip that can be broken to create an opening with an outer diameter of around 20 µm.
7. Heart injection needle: (Figure 2B) Create heart injection needles by pulling a glass capillary with a filament (10 cm length, 1.5 mm outer diameter, 0.86 mm inner diameter) to an inner tip diameter of 1–3 µm.
8. Fluid jet: (Figure 2C) Prepare fluid-jet needles by pulling a glass capillary without a filament (10 cm length, 1.5 mm outer diameter, 0.86 mm inner diameter) to create a long, tapered tip that can be broken to a tip diameter of 30–50 µm.
9. Larval manipulator (Figure 3A): Feed 2 lb fishing line through the 3 in long glass capillary and trim, leaving around 5 mm of fishing line exposed beyond each end of the capillary. Apply a dot of superglue to the two ends of the glass capillary to glue the fishing line to the capillary.

KEY RESOURCES TABLE

REAGENT or RESOURCE	SOURCE	IDENTIFIER
Chemicals, peptides, and recombinant proteins		
Tricaine (MS-222)	Pentair	TRS5
QIAprep Spin Miniprep kit	QIAGEN	27106
Low-melt agarose	Thermo Fisher Scientific	BP 165-25
Mineral oil	Thermo Fisher Scientific	S25439
N-methyl-D-aspartate (NMDA)	MilliporeSigma	M3262
Dow Corning® high vacuum grease	Sigma-Aldrich	Z273554
Alpha-bungarotoxin	R&D Systems	2133
Phenol red solution 0.5%	Sigma-Aldrich	P0290

(*Continued on next page*)

Continued

REAGENT or RESOURCE	SOURCE	IDENTIFIER
Experimental models: Organisms/strains		
Tg(5kbneurod:G-GECO)^{nl19} heterozygote zebrafish at 4 days post-fertilization (dpf); sex not determined at this stage	(Mandal et al., 2018)	ZDB-ALT-180628-5
AB wildtype zebrafish strain at 4 dpf; sex not determined at this stage	ZIRC	ZDB-GENO-960809-7
Recombinant DNA		
mnx1:SypHy-p2a-mRFP	(Mandal et al., 2020)	N/A
Software and algorithms		
Microscope software to for confocal imaging	ZEISS	Zen (Black edition)
ImageJ (FIJI)	National Institutes of Health	https://imagej.net/Fiji/Downloads
JMP15	JMP	https://www.jmp.com/en_us/software/data-analysis-software.html
Microscope software to simultaneously control confocal imaging and stimulation	Bruker	Prairieview 5.3
Other		
Micropipette puller	Sutter Instrument	Flaming/Brown Model P-97
Stage micrometer (1 mm with 0.01 div)	Thermo Fisher Scientific	1186Z70
35 mm dish with 10 mm hole punched lid	Custom	Custom
22 × 22 mm coverslip (#1.5)	VWR	48366-227
Stereo microscope	Carl Zeiss Microscopy	Stemi 2000 with transmitted light illumination
Epifluorescence stereo microscope; 83–100× magnification; GFP and mRFP filter sets; metal-halide light source	ZEISS	AxioZoom V1.6 with Hxp 200C illuminator
4.5 kg test (0.30 mm diameter) monofilament fishing line	Stren High Impact	SHIQS10-22
Borosilicate glass capillaries without filament (3 in length, 1.0 mm outer diameter)	World Precision Instruments	1B100-3
Forceps (#5 or #55)	Fine Science Tools	Dumont #5 (0.05 × 0.02 mm): 11295-10 Dumont #55 (0.05 × 0.02 mm): 11255-20
Borosilicate glass capillaries with filament (4 in length, 1.0 mm outer diameter)	World Precision Instruments	TW100F-4
Gel loading tips	Eppendorf	5242956003
Manual micromanipulator	NARISHIGE	M-152
Magnetic stand	NARISHIGE	GJ-1
Glass pipette/needle holder	WPI	MPH315
Glass Pasteur pipette	Chemglass Life Sciences	IP60 #5 3/4
Pipette pump dispenser	Bel-Art	F378980000
Zygote injection mold	Adaptive Science Tools	TU-1
Confocal laser scanning microscope with 488 nm and 561 nm lasers and appropriate filters	e.g., ZEISS	e.g., LSM800
63×/NA1.2 W objective	ZEISS	C-Apochromat 63×/1.20 W Corr UV-VIS-IR
10× air objective	ZEISS	EC Plan-Neofluar 10×/0.30 WD=5.2 M27
Swept-field confocal or similar with 488 nm laser and appropriate filters	Bruker	Swept field/Opterra confocal microscope
60×/NA 1.0 W dipping objective	Nikon	MRF07620
10× air objective	Nikon	MRH00101
Pressure clamp and head stage (HSPC-1)	ALA Scientific	HSPC-1 High-speed pressure Clamp with PV-PUMP
Pressure and vacuum pump	ALA Scientific	PV-Pump
Circular chamber adapter	Siskiyou	PC-A

(*Continued on next page*)

Continued

REAGENT or RESOURCE	SOURCE	IDENTIFIER
Motorized micromanipulator with microscope stage adaptor	Sutter Instrument Company	MP-225
Micromanipulator controller	Sutter Instrument Company	MPC-200
Masterflex Peroxide-cured silicone tubing (connects the fluid-jet needle holder to the pressure clamp/head stage)	Cole-Palmer	Masterflex L/S 13, 96400-13
PSI manometer	Sper Scientific	840081
Glass pipette/needle holder	WPI	MPH315
Ceramic tile	Sutter Instrument Company	NC9569052
Borosilicate glass capillaries with filament (10 cm length, 1.5 mm outer diameter, 0.86 mm inner diameter)	Sutter Instrument Company	BF150-86-10
Borosilicate glass capillaries without filament (10 cm length, 1.5 mm outer diameter, 0.86 mm inner diameter)	Sutter Instrument Company	B150-86-10
Pressure injector for heart injection	Eppendorf	Femtojet 4×

MATERIALS AND EQUIPMENT

0.4% tricaine (MS-222)

Reagent	Final concentration	Amount
ethyl 3-aminobenzoate methanesulfonate salt	0.4%	400 mg
Na_2HPO_4	0.8%	800 mg
distilled water	N/A	100 mL
Total	N/A	100 mL

Adjust the pH to 7. Aliquot and store at 4°C for up to 1 month. Dilute 0.4% tricaine in approximately 20× volume of E3 embryo media to achieve a working concentration of 0.02% tricaine for anesthetizing larvae during immobilization and α-bungarotoxin injection.

Note: Store ethyl 3-aminobenzoate methanesulfonate salt at −20°C.

E3 embryo media 20× stock solution

Reagent	Final concentration	Amount
NaCl	0.300 M	17.5 g
KCl	10.1 mM	0.75 g
$CaCl_2$	26.1 mM	2.9 g
$MgSO_4$	40.7 mM	4.9 g
KH_2PO_4	3.01 mM	0.41 g
Na_2HPO_4	0.845 mM	0.12 g
ultrapure water	N/A	fill to 1 L
Total	N/A	1 L

Heat briefly if solids do not dissolve. Store at 4°C for up to 6 months.

Sodium bicarbonate stock solution 500×

Reagent	Final concentration	Amount
$NaHCO_3$	500×	3 g
ultrapure water	N/A	100 mL
Total	N/A	100 mL

Store at 4°C indefinitely.

E3 embryo media 1× working solution		
Reagent	Final concentration	Amount
E3 embryo media 20× stock	1×	400 mL
Sodium bicarbonate 500× stock	1×	16 mL
ultrapure water	N/A	7,584 mL
Total	N/A	8 L

Final concentrations: 15.0 mM NaCl; 0.505 mM KCl; 1.31 mM $CaCl_2$; 2.04 mM $MgSO_4$. Store at 22°C–25°C for up to 6 months.

1.8% low-melt agarose		
Reagent	Final concentration	Amount
Low-melt agarose powder	1.8%	1.8 g
E3 embryo media	1×	100 mL
Total	N/A	100 mL

Make 2–5 mL aliquots and store at 4°C for up to 6 months. Melt the agarose in boiling water and let cool to 42°C prior to mounting larvae for imaging.

Note: Melted agarose may be cooled for storage and re-melted.

α -bungarotoxin		
Reagent	Final concentration	Amount
α-bungarotoxin	1%	1 mg
phenol red	3.3%	33.4 μL
ultrapure water	1×	968.6 μL
Total	N/A	1 mL

Make 100 μL aliquots and store at −20°C for up to one year.

⚠ CRITICAL: α-bungarotoxin is toxic. It is harmful in contact with skin and if inhaled. Wear gloves and use the hood when handling α-bungarotoxin powder.

STEP-BY-STEP METHOD DETAILS

Generation of transient transgenic larvae for SypHy expression in neurons

Timing: 6 h

This section describes the generation of zebrafish larvae with mosaic expression of the exocytosis indicator SypHy in neurons for the detection of synaptic vesicle release in the motor neuron presynapse.

1. Prepare an injection solution of 3–13 pg/nL plasmid DNA (*mnx1:SypHy-p2a-mRFP*) in deoxyribonuclease and ribonuclease-free water.
   a. Backfill 10 μL of plasmid solution into embryo injection needle.
   b. Insert the injection needle into a glass pipette holder clamped onto a micromanipulator.
2. For the first use of a plasmid, prepare injection solution with multiple plasmid concentrations to identify the optimal plasmid concentration.

   Note: The optimal concentration yields a sufficient percentage of expressing cells in the larvae for efficient analysis.

   a. Examine the injected larvae under a fluorescent stereo microscope to visualize transgene expression for identifying optimal plasmid concentration.

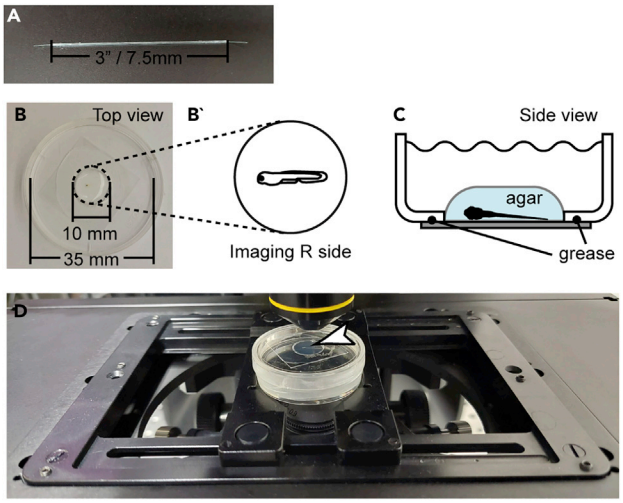

Figure 3. Zebrafish larva is embedded on a coverslip in agarose

(A) Fine embryo manipulator used in zebrafish transgenesis. Construction of this tool is described in step 9 of "Prepare needles for injection and embryo manipulators".

(B) Zebrafish larva is embedded in 1.8% low melt agarose held within the punched-out hole of a 35 mm petri dish, backed by 22 × 22 mm (#1.5) coverslip. In this view, you are looking down onto the agarose, with the cover slip below. The right side of the larva faces the coverslip. (B') In this example, the larva is positioned for imaging on the right side, which faces the coverslip.

(C) Schematic of larva placement in a side view of the bisected petri dish shows the larva (black) pressed on its side against the coverslip (gray), which is attached onto the petri dish by vacuum grease. The petri dish is filled with E3 to allow fluid exchange.

(D) Fully assembled imaging setup with the petri dish holder and petri dish, filled with embryo media, then closed and sealed with Parafilm around the edge. Within the petri dish, the larva is mounted against the coverslip such that the distance between the objective and the larva is minimized. Arrowhead indicates larva position.

Note: Once the optimal dose is identified, use this injection amount for all experiments to ensure expression consistency. Excess amount of plasmid introduced to the embryo can be lethal.

3. Using forceps, break the tip of the injection needle to create a tip opening diameter of around 20–25 μm, preferably with a beveled tip to effectively penetrate the chorion and embryo.
4. Calibrate droplet diameter to 120 μm for a 1 nL volume by suspending in mineral oil on micron slide (Drerup and Nechiporuk, 2016).
5. Collect zebrafish embryos within 20 min of spawning.
6. Microinject into single cell of zebrafish zygotes at the one cell stage.

Note: Zebrafish zygotes may be stabilized in a 1.5% agarose plate within troughs formed by a plastic mold (Adaptive Science Tools).

a. Incubate embryos in petri dishes filled with E3 embryo media at 50–100 embryos per dish in an incubator set to 28.5°C.
b. At 3–4 h post-fertilization, remove any unfertilized or abnormal embryos.
c. Continue to remove abnormal or dead embryos at least every other day starting at 1 dpf.

Generation of stable transgenic lines for G-GECO expression in neurons

Timing: 6 months

This section describes the generation of a novel zebrafish transgenic line with neuronal expression of the calcium indicator G-GECO. Completion of this section generates zebrafish larvae

expressing G-GECO in all neurons for the detection of calcium flux in the motor neuron presynapse.

Note: Instead of generating a new transgenic line, adults or embryos may be requested from laboratories maintaining the *Tg(5kbneurod:G-GECO)*^{nl19} transgenic line.

7. Prepare an injection solution of 7 pg/nL of *pDestTol2CG2-5kbneuroD:G-GECO* plasmid DNA along with 100 pg/nL Tol2 transposase mRNA in deoxyribonuclease and ribonuclease-free water.
   a. Backfill plasmid solution into embryo injection needle.
   b. Insert the injection needle into a glass pipette holder clamped onto a micromanipulator.

Note: Tol2 transposase mRNA is synthesized using an mMessage Machine SP6 kit (ThermoFisher catalog# AM1340). Store Tol2 transposase RNA in single use aliquots at −80°C to avoid freeze-thaw cycles.

8. Calibrate droplet diameter to 120 μm for a 1 nL volume suspended in mineral oil over micron slide.
9. Collect zebrafish embryos within 20 min of spawning.
10. Microinject into zebrafish zygotes at the one cell stage.
11. Screen injected embryos (F0) at 2–4 dpf for G-GECO expression in neurons of interest.

Note: Transgenesis will occur in a subset of the injected embryos and these embryos will show mosaic transgene expression.

12. Raise G-GECO expressing F0 embryos to reproductive maturity.
13. Outcross F0 transgenic zebrafish with wild type and screen the progeny embryos (F1) for transgene expression in neurons of interest.

Note: Since F0 zebrafish are mosaic for the transgene, a variable subset of their offspring will be heterozygous for the transgene.

14. Raise G-GECO expressing F1 embryos to reproductive maturity.
15. Outcross heterozygous F1 zebrafish to create heterozygous F2 zebrafish.
    a. Identify lines with a single transgenic insertion event by assessing larvae for transgene expression on a fluorescent stereo microscope.

Note: Mendelian inheritance with visually similar levels of transgene expression is indicative of single integration of the transgene. These F2 heterozygote zebrafish and their offspring can be used as stable transgenic larvae for calcium imaging experiments.

Image acquisition: Spontaneous motor neuron synaptic activity

Timing: 4–8 h

This section describes the imaging of spontaneous motor neuron synaptic vesicle release in the absence of stimuli using the fluorescent exocytosis indicator SypHy. Completion of this section will generate imaging data for measuring the rate of spontaneous motor neuron synaptic activity.

16. Raise zygotes injected with plasmid DNA encoding *mnx1:SypHy-p2a-mRFP* to 4 dpf.
    a. Sort larvae for expression of the mRFP reporter in the cell body of spinal motor neurons of the ventral spinal cord on a fluorescent stereo microscope.
    b. Because the objective recommended in this protocol for imaging has a limited working distance, make sure to group sorted larvae based on whether neurons expressing fluorescent

reporters are on the left or right side of the larvae by placing each group in a separate dish containing E3 embryo media.

Note: This step is to ensure that the side of the larva containing the motor neuron of interest will be mounted facing the objective.

17. Melt low melt agarose in water near boiling temperature and incubate in 42°C water bath to equilibrate.
18. Using vacuum grease, secure new coverslip to the top of the punched petri dish lid.
19. Anesthetize larvae in fresh E3 embryo media with 0.02% tricaine (0.4% tricaine diluted 1/20 in E3) and mount the larvae.
    a. Wash larvae briefly in fresh embryo media to remove the tricaine.
    b. Individually mount larvae in 1.8% low-melt agarose (Figures 3B and 3C).
        i. Use glass pipette to individually dispense larvae suspended in minimal volume of E3 into agarose.
        ii. Pipette the larvae, now suspended in agarose solution, onto coverslip mounted on 35 mm punched petri dish lid.
        iii. While the agarose is fluid, gently press the side of the larva with the expressing neuron onto the coverslip.

Note: Minimize the gap between the surface of the larva and coverslip using a fine embryo manipulator. The larva should lie on one side with the right and left eyes and horizontal myosepta appearing directly on top of one another when viewed from above. Embed the larvae in agarose within 1 min following the removal of tricaine before the anesthetic effect is lost.

⚠ CRITICAL: High percentage agarose is essential here to eliminate movement as larvae are no longer in anesthetic during imaging. A gap between the larva and the coverslip will significantly degrade signal intensity.

20. Once agarose has solidified (~1–2 min), submerge the solidified low-melt agarose in embryo media by placing the lid on the 35 mm petri dish bottom filled to the brim with embryo media (Figure 3D).
    a. Wrap edge with parafilm to avoid spillage.
21. Identify a motor neuron axon terminal of interest.
    a. Under brightfield or phase contrast illumination on a confocal microscope, identify the ventral spinal cord with a 10× objective.
    b. Add water for immersion to the coverslip.
    c. With a 63× (NA1.2) water immersion objective, identify the cell body of the targeted motor neuron using the cytosolic mRFP and trace its axon through the trunk to a terminal on the surface of the trunk, near the horizontal myoseptum (Figures 4A and 4B).
22. After identifying a motor neuron axon terminal of interest, adjust the focal planes for a z-stack of the region.
    a. Capture the mRFP and SypHy signal using 561 nm and 488 nm excitation lasers in an optimized z-resolution stack every 10 s for a total duration of 5 min, yielding 30 image stacks (Figures 4C–C‴, Methods video S1).

Note: We suggest that images be taken with optimal image parameters for best resolution dependent upon your confocal system. For the typical point-scanning confocal microscope, sequential imaging without averaging is ideal to allow sufficient temporal resolution while minimizing potential cross-talk by co-excitation between channels.

    b. Repeat for at least 10 animals for each group, subject to power analysis, to record spikes in SypHy signal indicative of spontaneous synaptic vesicle release.

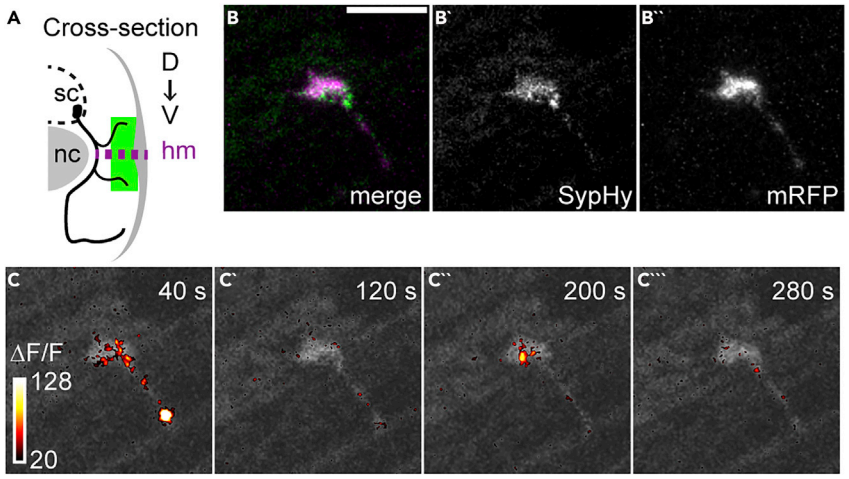

Figure 4. Zebrafish motor neuron with spontaneous synaptic vesicle release

(A) Schematic of the trunk cross-section showing the position of the notochord (nc), spinal cord (sc), and the primary motor neuron axons which extend from the spinal cord. Green rectangle on the horizontal myoseptum (hm, purple dotted line) represents the area and depth at which SypHy and mRFP signal are acquired from motor neuron axon to measure spontaneous motor neuron synaptic vesicle release.

(B) A representative image of an axon terminal of a motor neuron expressing SypHy (B′; green) and mRFP (B″; magenta). Scale bar = 5 μm.

(C) Over time, spontaneous synaptic vesicle release may be visualized within the motor neuron axon by increases in SypHy fluorescence intensity, indicated with a heatmap overlay.

⚠ CRITICAL: Keep all microscope settings (laser power, detector sensitivity and offset, etc) consistent between larvae imaged for the experiment.

Note: Because transient transgenesis generates reporter-expressing neurons in unpredictable locations, we select the CaP neuronal fiber that falls within the depth of the trunk denoted by the green box in Figure 4A. While the protocol presented here is used to analyze spontaneous motor neuron synaptic activity using SypHy, protocols described for stimulation-evoked motor neuron synaptic activity could be implemented to analyze evoked synaptic vesicle release (refer to G-GECO protocol below).

Optional: To augment synaptic vesicle release, spontaneous release frequency can be increased through incubation in 100 mM N-methyl-D-aspartate (NMDA). Previous work has shown NMDA treatment increased spontaneous motor neurons synaptic activity in fictive swimming behavior (Cui et al., 2004; McDearmid and Drapeau, 2006; Todd et al., 2004). Our previous work has shown that the effects of NMDA treatment on motor neuron is reflected in transient increases of motor neuron synapse SypHy fluorescence intensity (Mandal et al., 2020). This manipulation is valuable for questions regarding synaptic vesicle recycling or recruitment, which are required for sustained synaptic vesicle release.

Optional: To remove background SypHy fluorescence intensity resulting from exocytosis before the start of image acquisition, fluorescence recovery after photobleaching (FRAP) may be used by photobleaching the imaging area immediately prior to imaging in step 22. This procedure should be taken if the experiment involves the acute (e.g., pharmacological) rescue of exocytosis. In conditions where endocytosis is reduced, measurements of exocytosis using SypHy should also utilize FRAP. As an example, see (Koudelka et al., 2016).

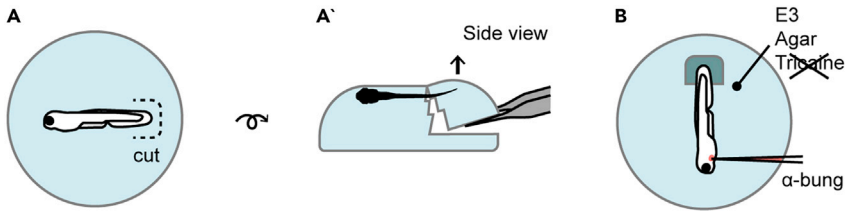

Figure 5. In order to produce evoked motor neuron synaptic activity, the tail of the zebrafish larva is freed from agarose to deliver tactile stimulation

(A) In preparation for stimulation, the tail is first freed from the agarose by cutting around the tail (A) and lifting the agarose free of the tail using #5 or #55 fine forceps (A′).

(B) Heart injection needle is used to deliver the paralytic α-bungarotoxin, which replaces tricaine, a sodium channel blocker. α-bungarotoxin eliminates muscle movement but does not alter neuronal activity. The heart injection needle must puncture through the low-melt agarose and enter the cardiac chamber from the ventral side of the zebrafish.

Image acquisition: Evoked motor neuron synaptic activity with fluid jet stimulation

Timing: 8 h

This section describes the imaging of evoked motor neuron synaptic calcium influx at the neuromuscular junction. Synaptic activity is evoked by stimulating the tail with a fluid jet. Completion of this section will generate imaging data for measuring the kinetics of calcium influx during synaptic activity at the motor neuron presynapse.

Note: This embryo mounting, and imaging method may also be used for live imaging of spontaneous activity.

23. Anesthetize larvae in fresh E3 embryo media with 0.02% tricaine (0.4% tricaine diluted 1/20 in E3) and mount the larvae.
    a. After movement ceases, position 4 dpf G-GECO expressing larva near the surface of a droplet of 1.8% low-melt agarose lying on one side, similar to the orientation described in step 19 above.
    b. Use fine forceps (#5 or #55) to cut two shallow lines parallel to each side of the tail (Figure 5A).
    c. Cut the agarose beneath the tail and lift the agarose that is bounded by the 3 cuts until it breaks off and slides off the tail (Figure 5A'). The caudal fin and some of the peduncle should be exposed.
    d. Submerge the larva in embryo media with 0.02% tricaine in order to immobilize the larva for heart injection.
24. Load needle with α-bungarotoxin for heart injection.
    a. Backfill heart injection needle with 3 μL α-bungarotoxin colored with phenol red used to visually confirm injection.
    b. Insert the heart injection needle to a pipette holder clamped to a micromanipulator next to a stereo microscope.
    c. Connect the pipette holder to a pressure injector with the following suggested settings: $P_{injection}$ = 100 hPa, $t_{injection}$ = 0.5 s, and $P_{compensation}$ = 5 hPa.
25. Position the pipette holder to point down ~30° from the horizontal and position the immobilized larvae such that the DV axis is parallel to the heart injection needle with the heart facing the needle.
26. On the stereo microscope, use the heart injection needle to penetrate the low-melt agarose and into the cardiac cavity.
    a. Inject one pulse into the cardiac cavity using the recommended pressure injector setting (Figure 5B). The cavity should distend slightly from the additional volume.

b. Rinse the paralyzed larva with 3 washes of embryo media to remove tricaine. Do not let the larva dry out during the rinses.

⚠ CRITICAL: Make sure the heart does not stop beating or significantly slow down. If the heartbeat is impacted, prepare a new larva.

27. Place the larvae under the objective of a confocal microscope with stimulation capability.
28. To prepare the fluid-jet needle for use in stimulation, backfill the fluid-jet needle with embryo media for fluid-jet stimulation.
    a. Create a wider opening for the fluid-jet needle by scoring the tip of the needle perpendicularly against a ceramic tile to break the tip such that the inner diameter of the opening is between 35 and 50 μm.

⚠ CRITICAL: Ensure that the break is even across the tip for well-directed flow.

29. Under phase contrast with a 10× objective of the confocal, position the fluid jet near the tail.
    a. Adjust the pressure output and visually confirm that the tail and tail fin are deflected without shifting the body of the larva (Methods video S2).
30. Set the back pressure such that the fluid jet pipette is not deflecting the tail at rest. Visually confirm by moving the pipette away from and back toward the tail; the tail should not move.
31. Locate somite 4, which may be identified by counting the chevron-shaped body segments that span the dorsal-ventral axis of the trunk (Figure 6A).
    a. Trace the motor neuron axon from the spinal cord until a superficially located bulbous axon terminal dorsal to the horizontal myoseptum but slightly ventral to the spinal cord is identified.
32. Switch to a 60× (NA 1.0) dipping objective and identify an imaging plane of interest.
33. Test the fluid-jet pressure to ensure that the imaging plane does not move out of focus during the application of fluid-jet stimulation.

⚠ CRITICAL: Movements which changes the focal plane (shifting in the Z axis) cannot be corrected post-acquisition with registration procedures. Minor shift in the imaging field of view (shifting in the X or Y axis) may be corrected by registration post-acquisition but should be minimized.

34. Capture the G-GECO signal at the single focal plane using a 488 nm excitation laser every 50 ms for a total duration of 10 s, yielding 200 images.
    a. Set the fluid jet to deliver a 50 ms pulse of fluid at 5 s (or 100 frames) after commencing image acquisition (Figures 6C–C‴, Methods video S3).
    b. Collect at least 12 measurements for each group.

⚠ CRITICAL: Multiple stimulation attempts should be separated by a 2 min rest period.

Note: Consistently selecting the area and tissue depth for imaging CaP axon in the G-GECO stable transgenic line improves signal consistency (Figure 6A). Even so, tail stimulation sometimes does not generate discernible G-GECO fluorescent intensity increase. Imaging trials with G-GECO intensity change <150% above the range of observed baseline fluorescence intensity (signal-to-noise ratio of 1.5×) may be discarded. In our experience, we have had difficulty identifying evoked G-GECO signal below this signal-to-noise threshold.

Note: Alternative protocol: Heart injection can be technically challenging. An alternative procedure to deliver α-bungarotoxin is to bathe the larvae in 50 μg to 1 mg/mL α-bungarotoxin in 0.5%–1% DMSO in E3 embryo media for ∼ 1 min (Randlett et al., 2015).

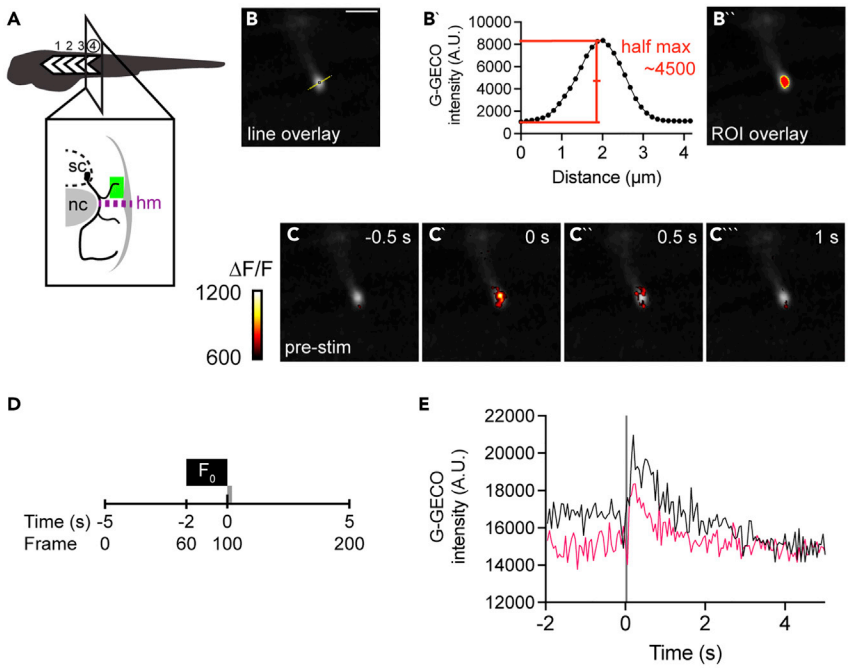

Figure 6. Zebrafish motor neurons with evoked presynaptic calcium influx

(A) Motor neuron axon calcium activity is recorded in the body segments 4–9, which are represented in this schematic as white chevrons. Starting from segment 4, a superficial area (green), dorsal to the horizontal myoseptum (hm, purple dotted line), but ventral to the spinal cord (sc), is imaged for G-GECO signal for evoked motor neuron axon calcium activity.

(B) In order to specify the region of interest (ROI) from which G-GECO fluorescence intensity is measured, an arbitrary straight line is drawn across the width of the imaged motor neuron axon. The signal intensity measured across the line is used to determine the half-max intensity (B′), which is used as the lower threshold limit (yellow outline) to define the pixels included in the measurement (red, B″). Scale bar = 5 µm.

(C) Evoked synaptic calcium activity may be visualized within the motor neuron axon immediately following the delivery of a tail stimulation, represented by increases in G-GECO intensity indicated with a heatmap overlay.

(D) Timeline of imaging events and corresponding frame number based on a framerate of 20 frames per s. Baseline intensity (F_0) is taken from the average of the 2-s (black bar) prior to stimulation delivery (gray bar).

(E) Two example traces of motor neuron axon G-GECO signal showing signal intensity increase immediately following stimulation onset (gray bar). Black trace is taken from the example show in (B-C‴). Pre-stimulation baseline intensity, peak intensity, and time-to-baseline can vary between axons.

Data analysis of spontaneous synaptic activity (SypHy) in motor neuron axon terminals using FIJI/ImageJ

Timing: 2–5 h

This section describes the procedure to measure spontaneous synaptic activity indicated by the fluorescent signal from the exocytosis indicator SypHy. Completion of this section will generate the relative rate of synaptic vesicle release at the motor neuron presynapse for comparison between groups.

Note: Most file format generated by software driving confocal microscopes may be opened by FIJI/ImageJ with the Bio-formats plugin.

35. In the FIJI tool bar, under "Analyze", use the "Set Measurement" window to select Area and Mean gray value as measurement values to display for analysis.
36. Import image sequence for analysis into FIJI.

37. Under "Image", in "Stack", use the "Z-project" function to generate sum-projected z-stacks of the axon terminal, excluding any focal planes above or below, through the time series.
    a. Using the freehand tool, outline the axon terminal to be analyzed.
    b. Moving through the stack, record the mean fluorescence intensity for the SypHy and mRFP channels separately.
38. To determine the average spontaneous synaptic activity over the time series, calculate the average mean fluorescence intensity of SypHy normalized to the mean fluorescence intensity of mRFP across entire time series and compare between groups.
39. Data sets can be compared using an ANOVA if the data is parametric or Wilcoxon rank sums for nonparametric data.
    a. Power analyses (use alpha = 0.05, beta = 0.2) should be done to confirm adequate sampling.

Data analysis of evoked synaptic activity in motor neuron axon terminals using FIJI/ImageJ

Timing: 2–5 h

This section describes the procedure to measure evoked synaptic activity indicated by the fluorescent signal from the calcium indicator G-GECO. Completion of this section will generate the kinetics of calcium influx at the motor neuron presynapse, from which the peak change can be extracted for comparison between groups.

40. In FIJI, install the Image Stabilizer plugin (Li, 2008). In the menu bar, under "Analyze", select the "Set Measurement" window, and check boxes for "Area", "Mean gray value", and "Add to overlay".
41. Import acquired images with FIJI.
42. Use the Image Stabilizer plugin to register X-Y movement artifacts.

Note: See Methods video S4 for a walkthrough of steps 42–46.

43. To segment the frame for intensity measurement, go to frame 60, or 3 s after imaging began, and draw a line region of interest (ROI) using the Straight-Line tool across an arbitrary axis of the visible motor neuron and include some background on each end of the line (Figure 6B).
    a. Under "Analyze", open the "Plot Profile" window to plot the intensity value across the line (Figure 6B').
    b. Calculate the average between the maximum and minimum intensity values. This half-max value will be used as the minimum threshold value to segment the image into regions (Figure 6B").
44. Use the threshold tool to segment the image from the half-max to the maximum value.
    a. Create an ROI around the area above the threshold using "Create selection" under "Edit", in the "Selection" sub header.
45. Open the "Roi manager" window and add the newly created ROI.
    a. In the "Roi manager", use "Multi measure" to record the values for the mean intensity for each time point on a spreadsheet, and record the area measured for this time series.
46. The ROI Manager window will contain the region(s) measured. In the ROI Manager, save the ROI containing the axon of interest. The saved file will be written in the .roi file format.
47. Plot the change in intensity over baseline.
    a. The baseline intensity (F_0) for each time series is generated by getting the average of the 2 s before stimulation (frame 60–99, Figures 6D and 6E).
    b. Calculate the change in intensity over baseline by subtracting fluorescence measurement (F) of each frame by F_0, and then divide this value by F_0 ($(F-F_0)/F_0$).
    c. From the change in intensity over baseline, collect the maximum value after stimulation onset for each time series.
48. Perform the appropriate statistical analysis on the peak change in intensity.

a. The distribution of peak change in intensity per experiment group is expected to approach Normal. If this holds true and variability between groups is consistent, data sets can be compared using ANOVA.

⚠ CRITICAL: If the distribution is non-normal, use Mann-Whitney U test for two sample tests or Kruskal-Wallis for multiple comparisons.

b. While sample sizes are typically 12 measurements per group, perform power analyses following collection to confirm adequate sampling.

Note: Currently, the amount of change in calcium activity necessary to represent physiological changes in presynaptic function is not known. It is therefore important to consider any reported differences in motor neuron presynaptic calcium activity in the context of changes in overall motor neuron function and behavioral output.

EXPECTED OUTCOMES

The expected outcome of imaging spontaneous motor neuron synaptic vesicle release with SypHy is the quantification of transiently expressed SypHy fluorescence intensity over an imaging area of a consistent size, normalized to mRFP intensity (Methods video S1). Pharmacological treatment such as NMDA has been shown to increase neuronal activity in the spinal cord of zebrafish (Cui et al., 2004; McDearmid and Drapeau, 2006; Todd et al., 2004). Using this treatment, we have seen an increase in the normalized SypHy intensity in wild type larvae (Mandal et al., 2020). The mean or sum normalized intensity from each imaging trial may be taken for statistical comparison of synaptic vesicle release between treatment groups.

From imaging evoked motor neuron synaptic activity with fluid jet stimulation, the expected outcome is the quantification of G-GECO fluorescence intensity over a region of image representing the visible axon (Methods video S3). G-GECO fluorescence intensity is expected to rise rapidly with tail stimulation, followed by an exponential decay to baseline after stimulation ends (Figure 6E). The measured G-GECO fluorescence intensity is normalized to the pre-stimulation baseline. The maximum intensity normalized to baseline from each imaging trial may be taken for the statistical comparison of presynaptic calcium activity between treatment groups. The average intensity normalized to baseline can also be plotted over time to show the kinetics of presynaptic calcium influx.

LIMITATIONS

In this protocol, we use CaP motor neurons in the larval zebrafish expressing genetically-encoded indicators to visualize motor neuron presynapse activity. When using transient transgenesis, indicator expression level should be sufficiently high, depending on the sensitivity of the detector, in order to capture images with low laser power, which will avoid tissue damage. Because the expression level in transient transgenesis can be unpredictable, extra zygotes should be injected to increase the likelihood of finding enough larvae for an experimental trial.

Using the approaches described above, it is possible to compare evoked and spontaneous neuronal activity in vivo between experimental groups. Because of the variability and sensitivity of these indicators and the temporal and spatial resolution of the described microscopy, results should be interpreted with caution. While comparing groups, e.g., experimental and control, can be done effectively, accurate levels of synaptic activity can be better studied using electrophysiological approaches.

While transient transgenesis is appropriate for indicators prone to express at high levels in neurons, some indicators, e.g., G-GECO, are not. If this is the case, stable transgenesis is essential to produce larvae with adequate and consistent expression for analysis.

TROUBLESHOOTING

Problem 1

Injected embryos do not express or weakly express transgene ("Generation of transient transgenic larvae" step 6).

Potential solution

If injected larvae, but not uninjected siblings, die between 1–2 dpf with opaque brain, reduce injected plasmid concentration.

If only a few larvae express and only in a few neurons within the larvae, first increase injected plasmid concentration. Also confirm consistent injection volume throughout injection session by recalibrating between injection rounds.

If these changes do not remedy the issue, recheck DNA quantity and quality using a spectrophotometer. Consider performing a new plasmid preparation to rule out plasmid quality issues.

Problem 2

When imaging larvae under a coverslip, unable to focus on the motor neuron axon, or neuron appears significantly dimmer under the microscope than viewed in binocular ("image acquisition: spontaneous motor neuron synaptic activity" step 21).

Potential solution

Larvae is positioned too far from the coverslip and new larvae should be mounted. Be sure to firmly press the trunk of the zebrafish on to the coverslip, minimizing any distance between the sample and the cover glass.

Problem 3

When introducing larvae to agarose, the larva darkens, curls, and the heartbeat stops ("image acquisition: spontaneous motor neuron synaptic activity" step 19 and "image acquisition: evoked motor neuron synaptic activity with fluid jet stimulation" step 23).

Potential solution

The agarose is too hot. Let the agarose cool to about 42°C before attempting to mount larvae.

Problem 4

G-GECO signal intensity appears as a sharp spike that returns to baseline intensity immediately following fluid jet stimulation without a gradual decay. ("image acquisition: evoked motor neuron synaptic activity with fluid jet stimulation" step 34).

Potential solution

The measured signal is a movement artifact (in the X Y or Z direction) and should be discarded. Smaller fluid jet needle opening diameter and positioning needle close to and above the tail with a lower pressure setting can reduce movement artifact.

Problem 5

Larva moves while under the microscope. ("image acquisition: spontaneous motor neuron synaptic activity" step 22 and "image acquisition: evoked motor neuron synaptic activity with fluid jet stimulation" step 34).

Potential solution

For spontaneous SypHy measurements, some movement is tolerable because the larva is embedded in relatively high concentration agarose that is quite stiff and limits the range of movement. The sum or average intensity data is also more tolerable to some degree of movement. For

evoked G-GECO measurements, larva movement will affect measurement interpretation. Inject the larva with a second dose of a-bungarotoxin and wait until visible movements subside before restarting the imaging session.

RESOURCE AVAILABILITY

Lead contact

Further information and requests for resources and reagents should be directed to and will be fulfilled by the lead contact, Catherine Drerup (drerup@wisc.edu).

Materials availability

Plasmids and zebrafish strains described in this protocol are available from the lead contact upon request.

Data and code availability

This study did not generate any unique datasets or code.

SUPPLEMENTAL INFORMATION

Supplemental information can be found online at https://doi.org/10.1016/j.xpro.2022.101766.

ACKNOWLEDGMENTS

This work was supported by the National Institute of Neurological Disorders and Stroke 1 R01NS124692-01 (C.M.D.) and by an Integrative Biology Post-degree Fellowship (H-T.C.W.). We would like to thank M. Chlebowski, A. Lang, C. Stein, and D. Mai for their thoughtful comments on the manuscript.

AUTHOR CONTRIBUTIONS

C.M.D. conceptualized the study. H.-T.C.W. designed the evoked imaging protocol, performed the experiments, analyzed the data, and wrote the paper. C.M.D. designed the spontaneous imaging protocol, performed the experiments, analyzed the data, and revised the paper.

DECLARATION OF INTERESTS

The authors declare no competing interests.

REFERENCES

Almeida, R.G., Williamson, J.M., Madden, M.E., Early, J.J., Voas, M.G., Talbot, W.S., Bianco, I.H., and Lyons, D.A. (2021). Myelination induces axonal hotspots of synaptic vesicle fusion that promote sheath growth. Curr. Biol. *31*, 3743–3754.e5. https://doi.org/10.1016/j.cub.2021.06.036.

Bello-Rojas, S., Istrate, A.E., Kishore, S., and McLean, D.L. (2019). Central and peripheral innervation patterns of defined axial motor units in larval zebrafish. J. Comp. Neurol. *527*, 2557–2572. https://doi.org/10.1002/cne.24689.

Berg, D.K., Kelly, R.B., Sargent, P.B., Williamson, P., and Hall, Z.W. (1972). Binding of alpha-bungarotoxin to acetylcholine receptors in mammalian muscle. Proc. Natl. Acad. Sci. USA *69*, 147–151. https://doi.org/10.1073/pnas.69.1.147.

Bernhardt, R.R., Chitnis, A.B., Lindamer, L., and Kuwada, J.Y. (1990). Identification of spinal neurons in the embryonic and larval zebrafish. J. Comp. Neurol. *302*, 603–616. https://doi.org/10.1002/cne.903020315.

Budick, S.A., and O'Malley, D.M. (2000). Locomotor repertoire of the larval zebrafish: swimming, turning and prey capture. J. Exp. Biol. *203*, 2565–2579. https://doi.org/10.1242/jeb.203.17.2565.

Campbell, R.E., Tour, O., Palmer, A.E., Steinbach, P.A., Baird, G.S., Zacharias, D.A., and Tsien, R.Y. (2002). A monomeric red fluorescent protein. Proc. Natl. Acad. Sci. USA *99*, 7877–7882. https://doi.org/10.1073/pnas.082243699.

Chang, C.C., and Lee, C.Y. (1963). Isolation of neurotoxins from the venom of Bungarus multicinctus and their modes of neuromuscular blocking action. Arch. Int. Pharmacodyn. Ther. *144*, 241–257.

Cui, W.W., Saint-Amant, L., and Kuwada, J.Y. (2004). Shocked gene is required for the function of a premotor network in the zebrafish CNS. J. Neurophysiol. *92*, 2898–2908. https://doi.org/10.1152/jn.00419.2004.

Drerup, C.M., and Nechiporuk, A.V. (2016). In vivo analysis of axonal transport in zebrafish. In Methods in Cell Biology (Elsevier), pp. 311–329. https://doi.org/10.1016/bs.mcb.2015.06.007.

Eisen, J.S., Myers, P.Z., and Westerfield, M. (1986). Pathway selection by growth cones of identified motoneurones in live zebra fish embryos. Nature *320*, 269–271. https://doi.org/10.1038/320269a0.

Fetcho, J.R. (1992). The spinal motor system in early vertebrates and some of its evolutionary changes. Brain Behav. Evol. *40*, 82–97. https://doi.org/10.1159/000113905.

Flanagan-Steet, H., Fox, M.A., Meyer, D., and Sanes, J.R. (2005). Neuromuscular synapses can form in vivo by incorporation of initially aneural postsynaptic specializations. Development *132*, 4471–4481. https://doi.org/10.1242/dev.02044.

Hale, M.E., Ritter, D.A., and Fetcho, J.R. (2001). A confocal study of spinal interneurons in living larval zebrafish. J. Comp. Neurol. *437*, 1–16. https://doi.org/10.1002/cne.1266.

Heckman, C.J., and Enoka, R.M. (2012). Motor unit. Compr. Physiol. *2*, 2629–2682. https://doi.org/10.1002/cphy.c100087.

Jontes, J.D., Buchanan, J., and Smith, S.J. (2000). Growth cone and dendrite dynamics in zebrafish

embryos: early events in synaptogenesis imaged in vivo. Nat. Neurosci. *3*, 231–237. https://doi.org/10.1038/72936.

Kim, J.H., Lee, S.-R., Li, L.-H., Park, H.-J., Park, J.-H., Lee, K.Y., Kim, M.-K., Shin, B.A., and Choi, S.-Y. (2011). High cleavage efficiency of a 2A peptide derived from porcine teschovirus-1 in human cell lines, zebrafish and mice. PLoS One *6*, e18556. https://doi.org/10.1371/journal.pone.0018556.

Kishore, S., Bagnall, M.W., and McLean, D.L. (2014). Systematic shifts in the balance of excitation and inhibition coordinate the activity of axial motor pools at different speeds of locomotion. J. Neurosci. *34*, 14046–14054. https://doi.org/10.1523/JNEUROSCI.0514-14.2014.

Koudelka, S., Voas, M.G., Almeida, R.G., Baraban, M., Soetaert, J., Meyer, M.P., Talbot, W.S., and Lyons, D.A. (2016). Individual neuronal subtypes exhibit diversity in CNS myelination mediated by synaptic vesicle release. Curr. Biol. *26*, 1447–1455. https://doi.org/10.1016/j.cub.2016.03.070.

Kwan, K.M., Fujimoto, E., Grabher, C., Mangum, B.D., Hardy, M.E., Campbell, D.S., Parant, J.M., Yost, H.J., Kanki, J.P., and Chien, C.-B. (2007). The Tol2kit: a multisite gateway-based construction kit for Tol2 transposon transgenesis constructs. Dev. Dyn. *236*, 3088–3099. https://doi.org/10.1002/dvdy.21343.

Lee, C.Y., Tseng, L.F., and Chiu, T.H. (1967). Influence of denervation on localization of neurotoxins from clapid venoms in rat diaphragm. Nature *215*, 1177–1178. https://doi.org/10.1038/2151177a0.

Li, K. (2008). The image stabilizer plugin for imageJ. http://www.cs.cmu.edu/~kangli/code/Image_Stabilizer.html.

Liu, Z., Chen, O., Wall, J.B.J., Zheng, M., Zhou, Y., Wang, L., Vaseghi, H.R., Qian, L., and Liu, J. (2017). Systematic comparison of 2A peptides for cloning multi-genes in a polycistronic vector. Sci. Rep. *7*, 2193. https://doi.org/10.1038/s41598-017-02460-2.

Mandal, A., Pinter, K., and Drerup, C.M. (2018). Analyzing neuronal mitochondria in vivo using fluorescent reporters in zebrafish. Front. Cell Dev. Biol. *6*, 144. https://doi.org/10.3389/fcell.2018.00144.

Mandal, A., Wong, H.-T.C., Pinter, K., Mosqueda, N., Beirl, A., Lomash, R.M., Won, S., Kindt, K.S., and Drerup, C.M. (2020). Retrograde mitochondrial transport is essential for organelle distribution and health in zebrafish neurons. J. Neurosci. *41*. JN-RM-1316-20. https://doi.org/10.1523/JNEUROSCI.1316-20.2020.

McDearmid, J.R., and Drapeau, P. (2006). Rhythmic motor activity evoked by NMDA in the spinal zebrafish larva. J. Neurophysiol. *95*, 401–417. https://doi.org/10.1152/jn.00844.2005.

Menelaou, E., and McLean, D.L. (2012). A gradient in endogenous rhythmicity and oscillatory drive matches recruitment order in an axial motor pool. J. Neurosci. *32*, 10925–10939. https://doi.org/10.1523/JNEUROSCI.1809-12.2012.

Miesenböck, G., De Angelis, D.A., and Rothman, J.E. (1998). Visualizing secretion and synaptic transmission with pH-sensitive green fluorescent proteins. Nature *394*, 192–195. https://doi.org/10.1038/28190.

Miledi, R., and Potter, L.T. (1971). Acetylcholine receptors in muscle fibres. Nature *233*, 599–603. https://doi.org/10.1038/233599a0.

Myers, P.Z., Eisen, J.S., and Westerfield, M. (1986). Development and axonal outgrowth of identified motoneurons in the zebrafish. J. Neurosci. *6*, 2278–2289. https://doi.org/10.1523/JNEUROSCI.06-08-02278.1986.

Palaisa, K.A., and Granato, M. (2007). Analysis of zebrafish sidetracked mutants reveals a novel role for Plexin A3 in intraspinal motor axon guidance. Development *134*, 3251–3257. https://doi.org/10.1242/dev.007112.

Randlett, O., Wee, C.L., Naumann, E.A., Nnaemeka, O., Schoppik, D., Fitzgerald, J.E., Portugues, R., Lacoste, A.M.B., Riegler, C., Engert, F., and Schier, A.F. (2015). Whole-brain activity mapping onto a zebrafish brain atlas. Nat. Methods *12*, 1039–1046. https://doi.org/10.1038/nmeth.3581.

Ryan, M.D., and Drew, J. (1994). Foot-and-mouth disease virus 2A oligopeptide mediated cleavage of an artificial polyprotein. EMBO J. *13*, 928–933. https://doi.org/10.1002/j.1460-2075.1994.tb06337.x.

Sankaranarayanan, S., De Angelis, D., Rothman, J.E., and Ryan, T.A. (2000). The use of pHluorins for optical measurements of presynaptic activity. Biophys. J. *79*, 2199–2208. https://doi.org/10.1016/S0006-3495(00)76468-X.

Seredick, S.D., Van Ryswyk, L., Hutchinson, S.A., and Eisen, J.S. (2012). Zebrafish Mnx proteins specify one motoneuron subtype and suppress acquisition of interneuron characteristics. Neural Dev. *7*, 35. https://doi.org/10.1186/1749-8104-7-35.

Todd, K.J., Slatter, C.A.B., and Ali, D.W. (2004). Activation of ionotropic glutamate receptors on peripheral axons of primary motoneurons mediates transmitter release at the zebrafish NMJ. J. Neurophysiol. *91*, 828–840. https://doi.org/10.1152/jn.00599.2003.

Zhao, Y., Araki, S., Wu, J., Teramoto, T., Chang, Y.-F., Nakano, M., Abdelfattah, A.S., Fujiwara, M., Ishihara, T., Nagai, T., and Campbell, R.E. (2011). An expanded palette of genetically encoded Ca^{2+} indicators. Science *333*, 1888–1891. https://doi.org/10.1126/science.1208592.